Journal of Plant Biology, September 2003, 46(3) : 187-198

Changes in Gene Expression during Hairy Root Formation by *Agrobacterium rhizogenes* Infection in Ginseng

Hwa-Jee Chung[1], In Sook Cho[1], Jee-Hyub Kim[2], Dong Su In[1], Cheol Goo Hur[2], Ji Sook Song[3], Sung Sick Woo[3], Dong-Woog Choi[1], and Jang Ryol Liu[1,4]*

[1]Laboratory of Functional Genomics for Plant Secondary Metabolism, Eugentech, Inc., Daejeon 305-333, Korea
[2]National Center for Genome Information, Korea Research Institute of Bioscience and Biotechnology (KRIBB), Daejeon 305-333, Korea
[3]Unigen, Inc. Cheonan, Chungnam 330-863, Korea
[4]Plant Cell Biotechnology Laboratory, Korea Research Institute of Bioscience and Biotechnology (KRIBB), Daejeon 305-333, Korea

Researchers have widely adopted the hairy root culture system as a means for producing secondary metabolites, including ginsenosides from ginseng. Although bacterial genes are involved, the aspects of plant gene expression are unclear. Using a cDNA microarray approach, we identified genes that are differentially expressed in ginseng hairy roots after *Agrobacterium rhizogenes* infection. Our goal was to gain an initial understanding of the correlation between hairy root morphology and ginsenoside production. Among the 250 genes analyzed here, 63 (including 14 that are unclassified) were differentially expressed in a hairy root line containing a high level of ginsenosides. Of the genes that had been functionally categorized, 29% and 17% were active in metabolism and stress responses, respectively. Most were primarily associated with ribosomal proteins, thereby functioning in protein synthesis and destination. Their expression was down-regulated in hairy roots having less lateral branching. This phenotype may have resulted from the manipulation of metabolic activities by the translational machinery.

Keywords: Araliaceae, ginsenosides, *Panax ginseng*, ribosomal protein genes

Panax ginseng C. A. Meyer (Araliaceae) is a very popular plant used as a sedative as well as an anti-fatigue and anti-diabetic traditional medicine (Sodati, 2000). Ginseng contains a mixture of triterpene saponins, or ginsenosides, as its major bioactive component. Because of high market demand, several culture systems have been widely adopted for the mass production of these ginsenosides (Canto-Canche and Loyola-Vargas, 1999; Bourgaud et al., 2001; Lian et al., 2002).

One system exploits the hairy roots induced by *Agrobacterium rhizogenes* infection to produce secondary metabolites, including ginsenosides. This technique has proven effective because it results in rapid growth and genetic stability without requiring growth hormones (Washida et al., 1998; Shanks and Morgan, 1999; Wu and Zhong, 1999; Giri and Narasu, 2000; Park and Facchini, 2000). *A. rhizogenes* contains a single copy of an Ri plasmid that carries one or more T-DNAs, similar to the Ti plasmids of *Agrobacterium tumefaciens*. The Ri plasmid T-DNA randomly integrates into the plant genome and induces hairy roots with morphological variations. Studies with *A. rhizogenes* and hairy root symptoms have demonstrated that two sets of genes in the Ri plasmid T-DNA region have a major role in the formation of hairy roots and the determination of root morphology. Three oncogenes that are harbored in the TL-DNA -- *rolA*, *rolB*, and *rolC* -- function in a synergistic way to induce these formations, whereas the *aux* genes in TR-DNA regulate hormone metabolism and root morphology (Amselem and Tepfer, 1992; Nilsson and Olsson, 1997; Tanaka et al., 1998). In addition to their function in hairy root formation, these two gene sets are also involved in producing secondary metabolites (Palazon et al., 1997, 1998; Bulgakov et al., 1998; Moyano et al., 1999; Bonhomme et al., 2000; Mallol et al., 2001). However, other than for the *rol* and *aux* genes, no reports have been made that correlate this production with either plant gene responses to T-DNA integration or hairy root formation.

DNA microarrays are an important tool for identifying genes and, simultaneously, characterizing differential gene expression patterns in various samples. The study described here constituted a pilot experiment using such a tool to explore the changes in gene expression that occur in hairy roots after *A. rhizogenes* infection.

*Corresponding author; fax +82-42-860-4608
e-mail jrliu@kribb.re.kr

By identifying distinctive expression profiles, we have attempted to reveal a possible relationship between ginsenoside production and the hairy root phenotype.

MATERIALS AND METHODS

Induction and Maintenance of Hairy Roots

Hairy roots of *P. ginseng* C. A. Meyer cv. Chunpung were induced from the cotyledons and petioles by infecting the seedlings with *A. rhizogenes* R1000 strain. Sterilized explants were cut into small pieces and immersed for 30 min in an *A. rhizogenes* culture suspended in a ½-strength MS liquid medium. The inoculated explants were then placed in the dark on 1/2 MS solid medium. After 2 d of co-cultivation, the explants were washed with 1/2 SH containing 800 mgL^{-1} cefotaxime, and transferred to a hormone-free 1/2 SH selection medium supplemented with 3% (w/v) sucrose, 0.4 mgL^{-1} thiamine HCl, 500 mgL^{-1} cefotaxime, and 2 gL^{-1} Gelrite. The explants were maintained on a 1/2 SH medium containing 100 mgL^{-1} cefotaxime until hairy roots emerged, and were later transferred onto an SH medium with 100 mgL^{-1} cefotaxime for mass propagation. The hairy root lines were maintained by sub-culturing on fresh media every four weeks.

RT-PCR Analysis

Total RNA was extracted, with a Qiagen RNeasy kit, from hairy roots grown on the SH medium. First-strand cDNA was synthesized using 25 to 250 ng of total RNA and a reverse transcriptase (Invitrogen). RT-PCR was conducted with gene-specific primers; amplification included 5 min of pre-denaturation at 95°C, followed by varying cycles of denaturation at 95°C for 30 s, annealing at 55°C for 30 s, and extension at 72°C for 60 s. The number of cycles were 32 for *aux*1 and 30 for *aux*2 and *rol*B. As a control, the ginseng 25S rRNA gene was amplified for 20 cycles. The sequences of the gene-specific primers were: *aux*1, 5'-ATG GCT GGA TCC TCC TTC ACA TTG C-3' and 5'-TCA CGC TTG ATA CCT ATA CCG CTT CC-3'; *aux*2, 5'-GAA AAT GGT GAC CCT CTC CTC GAT-3' and 5'-TTA CGA CAG AGT CGG ACG ATG CCT A-3'; *rol*B, 5'-CTT ATG ACA AAC TCA TAG ATA AAG GTT-3' and 5'-TCG TAA CTA TCC AAC TCA CAT CAC-3'; and 25S rRNA, 5'-TCA CCT GCC GAA TCA ACT AGC-3' and 5'-GAC TTC CCT TGC CTA CAT TG -3'.

cDNA Library and cDNA Microarray Preparation

PolyA$^+$ RNA was isolated from four-year-old ginseng roots according to the PolyAT tract mRNA isolation system (Promega). Afterward, a cDNA library was constructed using a cDNA synthesis kit (Stratagene, La Jolla, CA, USA), and ESTs were generated by mass excision from a phagemid library. A total of 1463 ginseng EST clones were then amplified by PCR (Multiblock System HT, MWG Biotech), using the T3 and T7 primers. PCR was performed in 40 μL of a reaction mixture containing 2 to 4 ng of DNA template, 10 x PCR buffer (500 mM KCl, 15 mM $MgCl_2$, 100 mM Tris [pH 8.8], 0.05% gelatin, and 3 mM DTT), 2.5 mM of dNTPs, 5 pmol of primers, and 0.5 units of Taq DNA polymerase. Conditions included 30 cycles of denaturation at 95°C for 30 s, annealing at 50°C for 30 s, and extension at 72°C for 1 min. The PCR products were analyzed on an agarose gel to check for a single band, and purified by centrifugation at 2000 rpm for 5 min, using a 96-well Millipore Multiscreen-HV plate (Sephadex g-50, Amersham Pharmacia). After drying, the DNA pellet was resuspended in 10 μL of TE (final concentration ~50 to 80 ng), and 4 μL of this resuspended solution was transferred to a 384-well microtiter plate containing 4 μL of spotting solution in each well (Telechem Co.). Amplified cDNAs were applied to silylated superamine substrates (ArrayitTM), using a printhead mounted with 16 pins of a SPH4B bubble pin (Telechem Co.) and a custom-built microarrayer (Gyeongsang University). After the slides were allowed to dry, they were UV-crosslinked with a UV 1800 Stratalinker (Stratagene) at 65 mJ cm^{-2}. Unbound DNA was removed by soaking the slides in 0.2% (w/v) SDS and washing them in double-distilled H_2O for 2 min. They were then denatured by boiling for 2 min, and dried for 5 min at room temperature. The slides were placed in a sodium borohydride solution (1 g $NaBH_4$ in 300 mL of PBS and 100 mL of 100% ethanol) for 5 min, washed three times in 0.2% SDS and double-distilled H_2O, then dried by centrifugation for 5 min at 500 *g*.

Preparation of Fluorescent Probes

First-stand cDNA was prepared as follows. An oligo (dT) 21-mer (1.5 μg) was annealed to 50 μg of total RNA by heating to 70°C for 5 min, then chilling on ice. Several components were added to the reaction mixture (40 μL total), including 5x first-strand buffer (GIBCO); 0.1 M DTT; 40 μL^{-1} of RNase inhibitor; 0.25 mM each of dATP, dGTP, and dCTP; 0.1 mM dTTP; 0.1 mM

cyanine 3 (Cy3)-dUTP or Cy5-dUTP (Amersham); and 200 μL^{-1} Superscript II reverse transcriptase (Gibco BRL). After incubating at 42°C for 2 h, the reaction tubes containing the Cy3- and Cy5-labeled probes were pooled and treated with 5 µL of 0.5 M EDTA and 10 µL of 1 N NaOH for 10 min at 37°C to degrade the RNA. Samples were neutralized by adding 25 µL of 1 M Tris-HCl (pH 7.5); the labeled single-stranded DNA was purified with a Millipore MC filter. The probe was precipitated with 0.1 volume of 3 M sodium acetate and 2 volumes of ethanol at −70°C for 15 min. Afterward, the pellet was washed with 70% ethanol, dried, and dissolved in a hybridization solution containing 6x SSC, 0.2% (w/v) SDS, 5x Denhardt solution (1% [w/v] Ficoll 400, 1% [w/v] polyvinylpyrrolidone, and 1% [w/v] bovine serum albumin [Sigma, Fraction V]) and 0.1 mg mL^{-1} salmon sperm DNA.

Hybridization and Scanning

The previously dissolved Cy3- and Cy5-labeled probes were boiled for 2 min, then rapidly applied to the microarray under a cover slip. Slides were placed in hybridization chambers and incubated for 12 to 16 h at 62°C. They were washed twice with 2x SSC, 0.2% SDS for 30 min, then with 0.05x SSC for 5 min. After the slides were dried by centrifugation, they were scanned for fluorescence emission using a Scan Array 3000 (GSI Lumonics). To normalize the two channels with respect to signal intensity, the ratios of the majority of the control genes were kept as close to 1.0 as possible. The average fluorescence was determined using the QuantArray program (GSI Lumonics). Background fluorescence was calculated as the median fluorescence signal of non-target pixels around each gene spot. Genes showing a signal value <1000 in both the Cy3 and Cy5 channels were not considered in this analysis.

Data Analysis

Gene-expression intensities of the tested hairy root lines were averaged from four independent experiments. For our clustering analysis of the microarray data, we selected 250 genes with average intensities of over ±0.2 log value. GeneSight Software (BioDiscovery) was used to generate hierarchical, K-means, and self-organizing maps (SOM) for these clusters. First, a Euclidean distance algorithm was applied to the genes and hairy root lines for hierarchical clustering. Because five groups were found here, we set the K value at 5 for K-means clustering, and performed SOM clustering as a map structure set on a 4 × 4 grid.

Chemicals and Reagents for HPLC Analysis

The reference ginsenosides Rb1, Rb2, Rc, Rd, Re, Rf, and Rg1 were purchased from INDOFINE Chemical Company, Inc. (Somerville, NJ, USA; purity >99%). A standard stock solution was prepared by dissolving 5 mg of each reference compound in 1 mL MeOH (1/1, v/v). This solution was stored at −15°C, and was diluted to the appropriate concentration for use in our qualitative confirmation. HPLC-grade acetonitrile was obtained from J.T. Baker (Deventer, The Netherlands), and our water was purified via a Milli-Q Plus System (Millipore; Milford, MA, USA)

HPLC Analysis

Twenty milligrams of the *P. ginseng* hairy roots was freeze-dried and powdered with liquid nitrogen. These lyophilized tissues were then extracted under sonication with 80% aqueous MeOH at 40°C for 1 h. The extract was centrifuged at 1000 rpm for 3 min, and the supernatant was evaporated under vacuum. This dried filtrate was then suspended in water and extracted with n-BuOH saturated with water. The n-BuOH layer was dissolved in MeOH (4000 ppm) after evaporation under vacuum, and 20°C of the sample was subjected to HPLC (4.6 × 250 mm Shiseido Capcell Pak MG column; ACN-H_2O gradient at flow rate of 1 mL min^{-1}; detection at 203 nm).

RESULTS AND DISCUSSION

Characterization of Hairy Root Phenotypes Used for cDNA Microarray Analysis

We produced over 100 individual hairy root lines, and selected 47 that showed no morphological variation over successive subcultures. These selected lines were grouped into five types, based on distinct root phenotypes (Fig. 1A). Types I and V included hairy roots that exhibited either a callus-like phenotype or fewer primary roots, respectively. Lines for Types II, III, and IV had long, thin primary roots, with diverse phenotypes in their lateral branching. About 40% of the hairy roots were of Type V; each of the other types comprised 13% to 17% of the samples. This diversity in morphology is commonly observed in many plant tissues, including cucumber and tobacco hybrids (Amselem and Tepfer, 1992; Moyano et al., 1999).

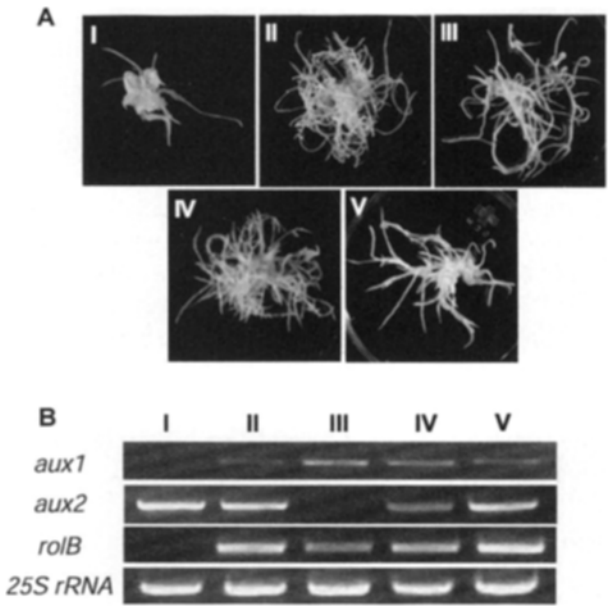

Figure 1. A, Various morphologies of *P. ginseng* hairy roots grown on an SH solid medium. **B,** Semi-quantitative RT-PCR profiles of *rol*B, *aux*1, and *aux*2 genes in hairy roots. 25S rRNA was used as a control.

Expression of the *rol* genes not only promotes hairy root formation, but also regulates the metabolism of plant hormones. By itself, *rol*B can significantly induce hairy roots (Nilsson and Olsson, 1997). The expression levels of *rol*B, *aux*1, and *aux*2 were determined in the hairy root lines via reverse transcription and polymerase chain reaction (RT-PCR) analysis (Fig. 1B). In Type I hairy roots, *rol*B expression was undetectable, while the other four types showed high transcript levels. For the *aux*1 gene, the highest expression was detected in the Type III hairy roots, followed, in order, by Types IV, V, and II. Again, this gene was not expressed in Type I hairy roots. Transcript of *aux*2 was found at similar levels for all hairy root types except Type III. To verify these transcript expression data, we used PCR to investigate the presence of the *rol*B, *aux*1, and *aux*2 genes in the genome of the hairy root lines, and found that all the hairy root types harbored our tested genes, except for *aux*2, which was absent in Type III (data not shown).

Analysis of Microarray Data

Based on the results described above, we proposed that the morphology of hairy roots might be determined through the interaction of the two microbial genes. However, we could not exclude the possibility that plant genes functioned in hairy root formation and metabolite production. To understand the plant response during that formation, we generated about 1500 EST clones from a cDNA library of four-year-old ginseng roots. These were amplified by PCR and printed on a glass slide. Using the callus-like Type I hairy root phenotype as a control, we compared the patterns of plant-gene expression in each hairy root type, with respect to its morphology and ginsenoside production. For our data analysis, EST clones were selected that had intense signals of over ±0.2 log value (Table 1). About 70% of the ESTs could be functionally classified; the remaining 30% were categorized as either unclassified proteins or proteins with unclear function. Among the classified ESTs, 28% were assigned to the category of protein synthesis, and 20% to metabolism. We applied three different clustering methods to the microarray expression data and compared their results before choosing a reliable biological pattern for differentiating the tested genes. Hierarchical clustering, using Euclidean distance, allowed us to visualize five clusters among the 250 ESTs. Based on this view, k-Means clustering analysis was performed with the K value set at 5. Nearly identical clustering patterns were generated by these two methods (data not shown). We then constructed SOMs set on a 4 × 4 grid for easy visualization of the detailed groupings (Fig. 2). Because the three clustering-analysis methods we applied showed consistent results, we analyzed the microarray data using SOMs to investigate and further differentiate gene expression in the hairy root lines.

Table 1. Selected genes showing an intense signal over ±0.2 Log value. Function annotation was from either Munich Information Center for Protein Sequences (MIPS) or the Gene Ontology Consortium

MIPS Category	Number of Genes
Metabolism	36
Energy	18
Cell growth, Cell division and DNA synthesis	4
Transcription	10
Protein synthesis	49
Protein destination	13
Transport facilitation	10
Cellular transport and Transport mechanisms	2
Cellular biogenesis	1
Cellular communication/Signal transduction	7
Cell rescue, Defense, Cell death and Aging	17
Cellular organization	8
Development	1
Transposable elements, Viral and Plasmid proteins	0
Classification not yet clear-cut	5
Unclassified proteins	69
Total	250

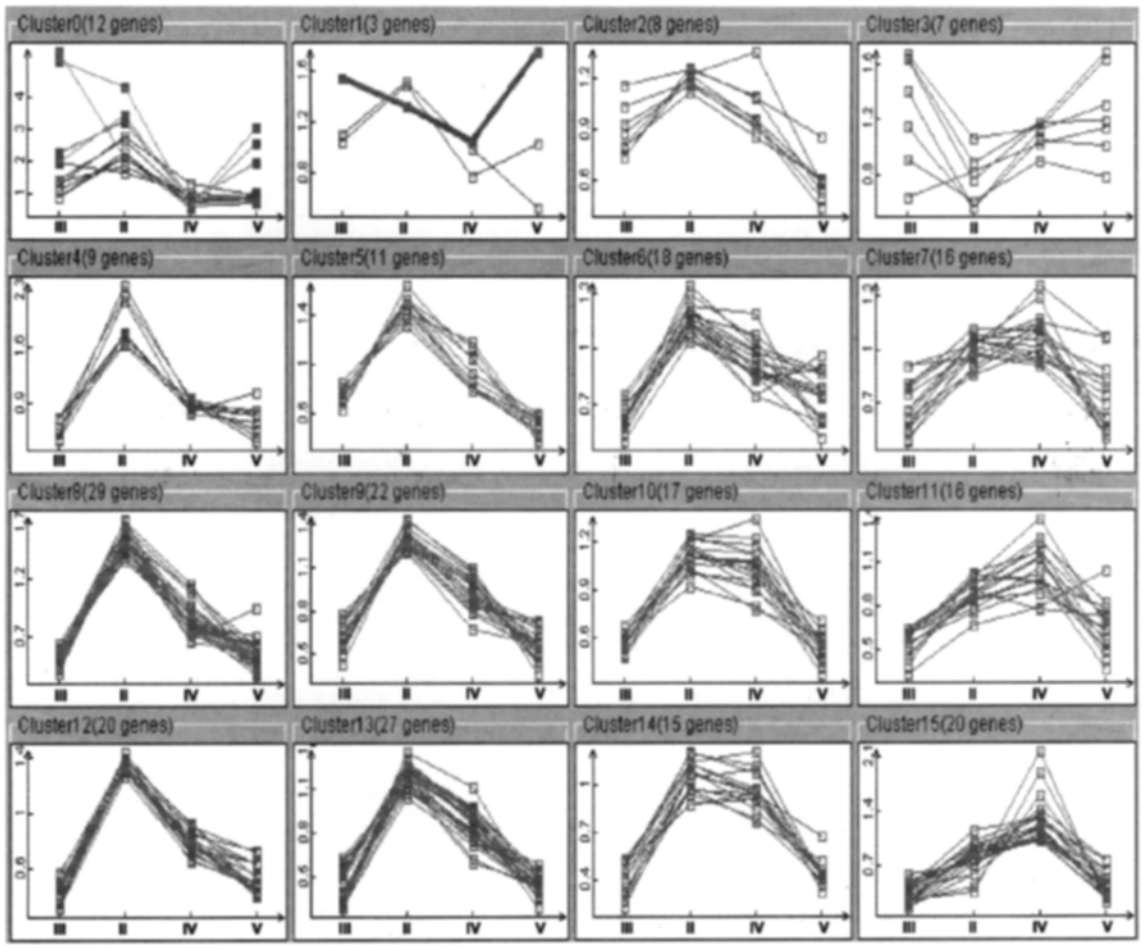

Figure 2. A self-organizing map (SOM) of gene expression in ginseng hairy roots. The 250 genes were grouped into 16 clusters using a 4 × 4 grid. Expression levels are shown on the y-axis; hairy root types, on the x-axis.

Gene Expression Profiles in Hairy Roots with Fewer Lateral Branches

Hairy roots of Types III and V had fewer lateral branches than those of Types II and IV. Therefore, we examined the clusters that exhibited a reduced level of gene expression in Types III and V simultaneously, and identified eight SOM clusters with significantly low levels of expression (Table 2). These clusters included genes that function in metabolism, energy, protein synthesis, protein destination, and cellular organization. Interestingly, 26% of these represented transcripts that encode ribosomal proteins (Fig. 3).

Ribosomes, which exist in all eukaryotes, are complex organelles composed of four ribosomal RNAs and about 80 different ribosomal proteins. In higher plants, expression levels of the latter are greatest in rapidly proliferating cells, including the shoot and root tips and the lateral root primordia (Williams and Sussex, 1995; Moran, 2000). Disruption of ribosomal proteins in *Arabidopsis* causes retarded root growth, aberrant leaf morphology, and embryo lethality, all outcomes that suggest their important role in plant growth and development (Ito et al., 2000; Weijers et al., 2001). Therefore, taken together with our observations here, the developmental process of lateral branch formation may require the expression of ribosomal protein gene sets.

Genes Differentially Expressed in Hairy Roots Producing High Levels of Ginsenosides

After total ginsenosides were extracted from the hairy roots, four of the protopanaxadiol type and three of the protopanaxatriol type were quantified through HPLC (Fig. 4). Type II hairy roots contained the highest level of ginsenosides, followed by Type V. The ratio between the protopanaxadiol-type ginsenosides (Rb1, Rb2, Rc, Rd) and the protopanaxatriol-type ginsenosides (Rg1,

Table 2. Genes with reduced RNA levels in hairy root lines showing less lateral branches. [a]Function annotation was from either Munich Information Center for Protein Sequences (MIPS) or the Gene Ontology Consortium.

EST ID	Description	Function[a]
Cluster 8		
HJ01001A06	gb|AAA33857.1| (M62758) S-adenosylmethionine synthetase	metabolism
HJ01021F12	gb|AF058955.1|AF058955 Mus musculus ATP-specific succinyl-CoA synthase	metabolism
PG03014F11	emb|CAA79702.2| (Z21493) mitochondrial formate dehydrogenase precursor	metabolism
PG03019D01	emb|CAB58175.1| (X74225) putative pod-specific dehydrogenase SAC25	metabolism
PG03020E07	emb|CAA56812.1| (X80840) homology to pyroxidal-5'-phosphate-dependant glutamate decarboxylases	metabolism
PG03022G11	ref|NP_194074.1| (NC_003075) putative protein	metabolism
PG03004E03	emb|CAC00532.1| (AJ132580) enolase, isoform 1	energy
PG03011C10	dbj|BAA33801.1| (AB018410) cytosolic phosphoglycerate kinase 1	energy
PG03012B08	emb|CAB39974.1| (AJ133422) glyceraldehyde-3-phosphate dehydrogenase	energy
HJ01002D11	ref|NP_000985.1| (NM_000994) 60S ribosomal protein L32	protein synthesis
HJ01004F09	gb|AAK43709.1|AF358665_1 (AF358665) ribosomal protein L32	protein synthesis
HJ01007G06	emb|CAA06491.1| (AJ005346) 40S ribosomal protein S5	protein synthesis
HJ01021D06	gb|AAA53296.1| (L18908) 60S ribosomal protein L25	protein synthesis
PG03002B12	gb|AAL47388.1| (AY064683) unknown protein	protein synthesis
PG03014C10	gb|AAD56018.1|AF180758_1 (AF180758) 60S ribosomal protein L10	protein synthesis
PG03021B07	emb|CAA36190.1| (X51910) GOS2	protein synthesis
HJ01004C04	dbj|BAA84650.1| (AB025310) asparaginyl endopeptidase	protein fate
PG03015H06	gb|AAA86089.1| (U17250) ubiquitin conjugating enzyme, E2	protein fate
PG03017E09	emb|CAA59963.1| (X85974) subtilisin-like protease	protein fate
PG03015D12	gb|AAC37402.1| (L28713) Ran protein/TC4 protein	transport facilitation
PG03010C08	gb|AAK06847.1| (AF332565) VirF-interacting protein FIP1	cell rescue and defense
HJ01002C12	gb|AAK96884.1| (AY054693) beta tubulin	cellular organization
PG03024H08	emb|CAA73171.1| (Y12599) histone H1	cellular organization
PG03001C04	gb|AAG33924.1| (AY009094) auxin-repressed protein	unclassified
HJ01021H12	gb|AAF18668.1|AC007168_1 (AC007168) unknown protein	unclassified
PG03014F10	gb|AAK18619.1|AF352797_1 (AF352797) ankyrin-repeat protein HBP1	unclassified
PG03015F03	gb|AAG53944.1| (AF304461) quinone-oxidoreductase QR1	unclassified
Cluster 9		
PG03011A06	ref|NP_199783.1| (NC_003076) cellulase homolog OR16pep precursor	metabolism
HJ01009C02	emb|CAC01238.1| (AJ292768) RNA Binding Protein 47	transcription
HJ01014B01	gb|AAA92861.1| (L47221) eukaryotic initiation factor 5	protein synthesis
PG03004A04	dbj|BAA19798.1| (D83527) YK426	protein synthesis
PG03006D02	gb|AAK25758.1|AF334838_1 (AF334838) ribosomal protein L17	protein synthesis
PG03011D07	gb|AAB68395.1| (U87222) elongation factor 1-beta	protein synthesis
PG03013A06	ref|NP_180719.1| (NC_003071) 40S ribosomal protein	protein synthesis
PG03016G02	dbj|BAA07207.1| (D38010) ribosomal protein S8	protein synthesis
PG03017F02	ref|NP_199687.1| (NC_003076) 60S ribosomal protein L13a	protein synthesis
PG03001G11	emb|CAA66481.1| (X97907) transcription factor	cellular organization
HJ01004F11	ref|NP_180162.1| (NC_003071) unknown protein	unclassified
PG03014F07	emb|CAC19848.1| (AJ252064) zfwd2 protein	unclassified
Cluster 10		
HJ01014B03	gi|228455|prf||1804333C Gln synthetase	metabolism
HJ01019C02	gb|AAD39534.2| (AF150630) cellulose synthase catalytic subunit	metabolism
PG03016F03	ref|NP_173289.1| (NC_003070) 60S ribosomal protein L6, putative	protein synthesis
PG03020F02	gb|AAD50774.1|AF161704_1 (AF161704) 40S ribosomal protein S17	protein synthesis
PG03021E02	ref|NP_176352.1| (NC_003070) ribosomal protein	protein synthesis
PG03006E06	ref|NP_190230.1| (NC_003074) ubiquitin conjugating enzyme E2 (UBC13)	protein fate
PG03016E06	ref|NP_175202.1| (NC_003070) serpin, putative	protein fate
PG03010D04	sp|P42055|POR4_SOLTU 34 Kda outer mitochondrial membrane protein porin	transport facilitation
PG03007E02	ref|NP_194088.1| (NC_003075) phosphatase like protein	signal transduction
PG03020C10	gb|AAB65162.1| (AF002667) heat shock cognate protein	cell rescue and defense
PG03001E12	ref|NP_178077.1| (NC_003070) unknown protein	unclassified
PG03022F08	ref|NP_172796.1| (NC_003070) unknown protein	unclassified
Cluster 11		
PG03011F12	ref|NP_192880.1| (NC_003075) putative protein	metabolism
PG03024C06	dbj|BAA03710.1| (D16139) cytokinin binding protein CBP57	metabolism
PG03020G09	gb|AAL09401.1|AF307336_1 (AF307336) ribosomal protein	protein synthesis
PG03020F09	emb|CAB72130.1| (AJ249331) heat shock protein 70	cell rescue and defense
PG03020B12	sp|P93436|ADHX_alcohol dehydrogenase class III (glutathione-dependent formaldehyde dehydrogenase)	unclassified

Table 2. Continued

EST ID	Description	Function[a]
Cluster 12		
HJ01014E04	gb|AAA20112.1| (M73430) S-adenosyl methionine synthetase	metabolism
PG03002C06	ref|NP_176527.1| (NC_003070) reductase, putative	metabolism
HJ01018F10	emb|CAA63598.1| (X93015) glyoxysomal beta-ketoacyl-thiolase	energy
PG03010H10	emb|CAA42905.1| (X60347) glyceraldehyde 3-phosphate dehydrogenase	energy
HJ01007A07	gb|AAD34458.1| (AF135596) Skp1	cell growth and division
HJ01001E09	ref|NP_200539.1| (NC_003076) 60S acidic ribosomal protein P3	protein synthesis
HJ01017F02	gb|AAB63814.1| (L46848) acidic ribosomal protein P0	protein synthesis
PG03001A06	ref|NP_201552.1| (NC_003076) 60S ribosomal protein L26	protein synthesis
PG03006H11	gb|AAB01095.1| (U47095) putative ribosomal protein	protein synthesis
PG03007D03	ref|NP_198801.1| (NC_003076) 40S ribosomal protein S9-like	protein synthesis
HJ01019A01	gb|AAF73016.1|AF262934_1 (AF262934) ubiquitin conjugating protein	protein destination
PG03004D05	sp|O22342|ADT1_ADPATP carrier protein 1 precursor (ADP/ATP translocase1)	transport
PG03023H06	gb|AAD28242.1|AF121355_1 (AF121355) peroxiredoxin TPx1	cell rescue and defense
PG03001D11	ref|NP_200010.1| (NC_003076) sorbitol dehydrogenase-like protein	unclassified
PG03003D05	sp|Q9XG77|PSA6_TOBAC Proteasome subunit alpha type 6	unclassified
PG03007B02	ref|NP_174096.1| (NC_003070) hypothetical protein	unclassified
Cluster 13		
HJ01003C04	gb|AAA33857.1| (M62758) S-adenosylmethionine synthetase	metabolism
HJ01013F01	ref|NP_172648.1| (NC_003070) lactoylglutathione lyase-like protein	energy
PG03019B01	gb|AAB38500.1| (U79767) methionine adenosyltransferase	enegry
PG03003C07	ref|NP_178224.1| (NC_003071) putative aldolase	transcription
PG03007A10	ref|NP_172537.1| (NC_003070) ATP citrate-lyase, putative	protein synthesis
HJ01018G04	gb|AAL06644.1| (AY048861) putative quinone oxidoreductase	protein synthesis
PG03002H09	sp|P50345|RLA0_LUPLU 60S acidic ribosomal protein P0	protein synthesis
PG03003B05	gb|AAC24585.1| (AF071891) 40S ribosomal protein S4	protein synthesis
PG03008D12	gb|AAB71079.1| (U62752) acidic ribosomal protein P1a	protein synthesis
PG03013H06	sp|Q40471|IF49_TOBAC eukaryotic initiation factor 4A-9	protein synthesis
PG03016A07	ref|NP_188229.1| (NC_003074) putative ribosomal protein	protein synthesis
PG03016D01	ref|NP_473288.1| (NC_000521) 40S Ribosomal protein S11	protein synthesis
PG03017D04	ref|NP_181874.1| (NC_003071) 60S ribosomal protein L38	protein fate
HJ01021C05	ref|NP_179311.1| (NC_003071) putative ubiquitin-like protein	protein fate
PG03023E03	gb|AAB51386.1| (U92087) stress responsive cyclophilin	transport
HJ01001H03	ref|NP_191788.1| (NC_003074) ADP-ribosylation factor-like protein	transport
PG03006G07	sp|P09469|VATA_DAUCA Vacuolar ATP synthase catalytic subunit	cell rescue and defense
HJ01001H10	emb|CAA32643.1| (X14482) manganese superoxide dismutase preprotein	cellular organization
HJ01002G10	ref|NP_178970.1| (NC_003071) putative chromodomain-helicase-	cellular organization
HJ01022E07	emb|CAA78483.1| (Z14110) actin depolymerizing factor	cellular organization
PG03005B10	gb|AAF89964.1|AF200528_1 (AF200528) cellulose synthase-4 DNA-binding protein	cellular organization
PG03001D04	gb|AAD24540.1|AF113545_1 (AF113545) vacuole-associated annexin VCaB42	unclassified
HJ01004A12	ref|NP_191340.1| (NC_003074) putative protein	unclassified
HJ01022C01	ref|NP_181438.1| (NC_003071) unknown protei	unclassified
PG03002E10	ref|NP_195125.1| (NC_003075) putative protein	unclassified
PG03023B07	ref|NP_197643.1| (NC_003076) alkaline/neutral invertase	
Cluster 14		
PG03016A11	emb|CAC39216.1| (AJ318053) glutamine synthetase	metabolism
PG03016C01	dbj|BAA34112.1| (AB019327) NADP specific isocitrate dehydrogenase	metabolism
PG03015E12	gb|AAC50019.1| (U39747) high mobility group protein 2 HMG2	transcription
HJ01015C09	emb|CAB65281.1| (AJ248327) L3 Ribosomal protein	protein synthesis
PG03003D12	ref|NP_196772.1| (NC_003076) elongation factor 1B alpha-subunit	protein synthesis
PG03014A12	emb|CAB09900.1| (Z97178) elongation factor 2	protein synthesis
PG03020G01	emb|CAA55047.1| (X78213) 60s acidic ribosomal protein P2	protein synthesis
PG03011E01	ref|NP_171732.1| (NC_003070) cathepsin B, putative	protein fate
PG03001C09	gb|AAG24642.1|AF308737_1 (AF308737) J1P	cell rescue and defense
PG03010H09	dbj|BAB67894.1| (AP003231) putative HSP70	cell rescue and defense
HJ01001F08	ref|NP_520651.1| (NC_003295) probable tetraacyldisaccharide 4 kinase protein	unclassified
PG03013E10	gb|AAF76227.1|AF272573_1 (AF272573) 14-3-3 protein	unclassified
PG03021F07	emb|CAA48892.1| (X69139) protease inhibitor II	unclassified
PG03021G11	gb|AAL06644.1| (AY048861) putative quinone oxidoreductase	unclassified

Table 2. Continued

EST ID	Description	Function[a]
Cluster 15		
HJ01019C04	sp|Q9AXE3|DCAM_ S-adenosylmethionine-decarboxylase proenzyme	metabolism
PG03002H10	gb|AAB80696.1| (U86072) omega-6 fatty acid desaturase	metabolism
PG03013D08	ref|NP_198892.1| (NC_003076) glucose-6-phosphate dehydrogenase	metabolism
PG03014E09	emb|CAA65200.1| (X95965) CER1-like	metabolism
PG03015B06	ref|NP_186847.1| (NC_003074) putative dehydrogenase	metabolism
PG03015C06	gb|AAB71213.1| (U82011) methyltransferase	metabolism
PG03023H01	ref|NP_199252.1| (NC_003076) berberine bridge enzyme-like protein	metabolism
PG03022E03	gb|AAB69318.1| (AF012862) cytosolic glucose-6-phosphate dehydrogenase 1	energy
HJ01003B03	dbj|BAA87070.2| (AB035272) TAT-binding protein homolog	protein fate
PG03016F11	dbj|BAA94511.1| (AB041505) ABC transporter homolog	transport
PG03017F03	ref|NP_187337.1| (NC_003074) acetyl-coA dehydrogenase, putative	transport
PG03008D07	gb|AAB61671.1| (AF005278) type IIIa membrane protein cp-wap11	cellular biogenesis
PG03021G10	gb|AAB80697.1| (U86374) fungal elicitor-induced protein	cell rescue and defense
PG03014H11	gb|AAC14179.1| (AF054445) major latex protein homolog	cell rescue and defense
PG03007E03	ref|NP_197478.1| (NC_003076) tubulin alpha-5 chain-like protein	cellular organization
PG03022D01	dbj|BAB40141.1| (AB058678) plasma membrane intrinsic protein 2-1	cellular organization
PG03005G08	gb|AAB88876.1| (U93273) putative auxin-repressed protein	unclassified
PG03006A05	ref|NP_190682.1| (NC_003074) putative protein	unclassified

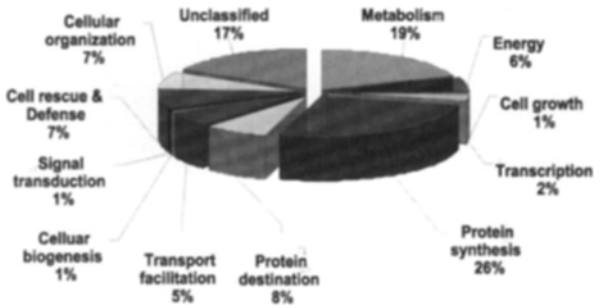

Figure 3. Relative abundance of functionally categorized genes in Types II and IV hairy roots. A total of 130 genes from Table 2 are included. Functional annotation was from either the Munich Information Center for Protein Sequences (MIPS) or the Gene Ontology Consortium.

Re, Rf) in each type ranged from 0.59 to 0.98.

In identifying the genes that might be correlated with ginsenoside production, we found that expression levels were highest in the Type II hairy roots (Table 3). In that group, 31% of the genes were involved in cell rescue and defense function; many encoded heat shock proteins (hsps). We identified four members of the hsp70 family, one hsp90 gene, one hsp110 gene, and one for low-molecular-weight hsp17. In comparison, *Arabidopsis* contains 7 members of the hsp90 family and 14 members of the hsp70 family (Milioni and Hatzopoulos, 1997; Sung et al., 2001). Expression profiles for 11 of the hsp70s have revealed that, except for a few members, they are induced by heat and/or cold stresses. Moreover, hsp70s may have prominent roles in root growth (Sung et al., 2001). Research with geldanamycin, which inhibits hsp90 function, has demonstrated that

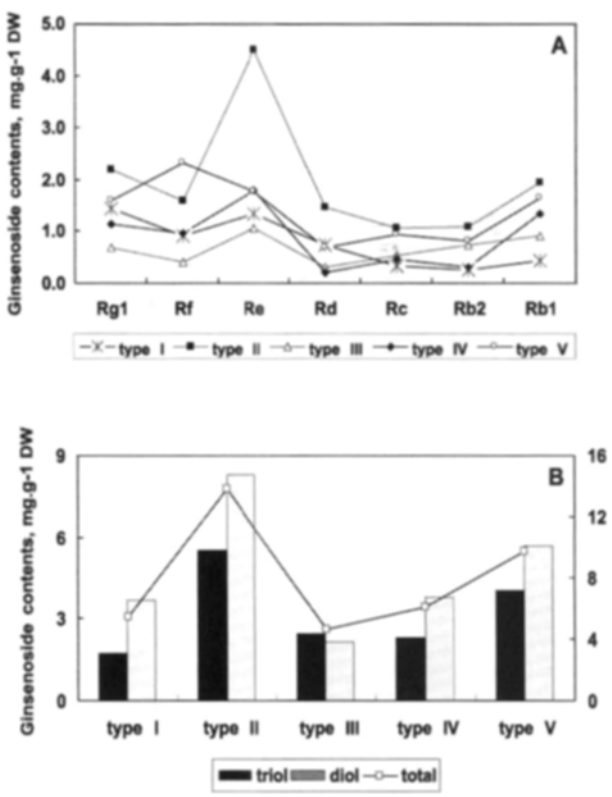

Figure 4. Ginsenoside in hairy root lines contents were quantified by HPLC from 6 to 19 lines of each respective phenotype, and are expressed as averages. Roots were subcultured every four weeks. Open bar indicates total content of protopanaxadiol-type ginsenosides, Rb1, Rb2, Rc, and Rd; closed bar indicates total content of protopanaxatriol-type ginsenosides Rg1, Rf, and Re. Line with triangle indicates total ginsenoside content of each hairy root line.

Table 3. Genes induced in type II hairy roots. [a] Function annotation was from either Munich Information Center for Protein Sequences (MIPS) or the Gene Ontology Consortium

EST ID	Description	Function[a]
PG03003E05	emb|CAB85625.1| (AJ237985) putative ripening-related protein	metabolism
PG03014F11	emb|CAA79702.2| (Z21493) mitochondrial formate dehydrogenase precursor	metabolism
PG03022G11	ref|NP_194074.1| (NC_003075) putative protein	metabolism
HJ01003A10	ref|NP_200158.1| (NC_003076) NADH-dependent glutamate synthase	energy
HJ01003E12	gb|AAF85975.1|AF275639_1 (AF275639) cytosolic phosphoglycerate kinase	energy
HJ01010D01	gb|AAG22488.1|AF195868_1 (AF195868) pyruvate decarboxylase 1	energy
PG03004E03	sp|Q9LEJ0|ENO1_enolase 1 (2-phosphoglycerate dehydratase 1)	energy
PG03012B08	emb|CAB39974.1| (AJ133422) glyceraldehyde-3-phosphate dehydrogenase	energy
PG03007B03	ref|NP_177907.1| (NC_003070) eukaryotic initiation factor 5 (eIF-5), putative	protein synthesis
HJ01004C04	dbj|BAA84650.1| (AB025310) asparaginyl endopeptidase	protein fate
HJ01010G03	pir||T03251 calnexin - maize (fragment)	protein fate
PG03017E09	pir||S52770 subtilisin-like proteinase (EC 3.4.21.-), nodule-specific	protein fate
PG03006C02	gb|AAB65162.1| (AF002667) heat shock cognate protein	cell rescue and defense
PG03022A11	gb|AAF34134.1| (AF161180) high molecular weight heat shock protein	cell rescue and defense
HJ01002A11	pir||S25005 dnaK-type molecular chaperone precursor, mitochondrial- kidney bean	cell rescue and defense
HJ01015C06	emb|CAA68885.1| (Y07613) heat shock protein 90A	cell rescue and defense
HJ01018B12	sp|P27396|HS11_17.8 KD class I heat shock protein	cell rescue and defense
PG03016H11	gb|AAG16758.1| (AY007560) putative glutathione S-transferase T3	cell rescue and defense
PG03007C02	ref|NP_178111.1| (NC_003070) putative heat-shock protein	cell rescue and defense
PG03008B03	ref|NP_192897.1| (NC_003075) phospholipid hydroperoxide glutathione peroxidase	cell rescue and defense
PG03022C09	pir||S53126 dnaK-type molecular chaperone hsp70 rice	cell rescue and defense
PG03019B08	pir||T03684 phosphoprotein phosphatase (EC 3.1.3.16) 2A regulatory chain	signal transduction
HJ01004E03	gb|AAD41039.1|AF112538_1 (AF112538) actin	cellular organization
PG03024H08	emb|CAA73171.1| (Y12599) histone H1	cellular organization
HJ01012B01	ref|NP_181942.1| (NC_003071) unknown protein	unclassified
HJ01021H12	gb|AAF18668.1|AC007168_1 (AC007168) unknown protein	unclassified
PG03001B12	ref|NP_199660.1| (NC_003076) putative protein	unclassified
PG03012G07	emb|CAA59472.1| (X85206) hybrid proline-rich protein	unclassified
PG03024F12	gb|AAG33924.1| (AY009094) auxin-repressed protein	unclassified

the protein affects developmental plasticity but allows morphogenetic variation in response to the environment (Queitsch et al., 2002). Although these studies provide evidence of a link between environmental changes and plant growth and development, as regulated by heat shock proteins, no reports have been made on the relationship between those proteins and metabolite production.

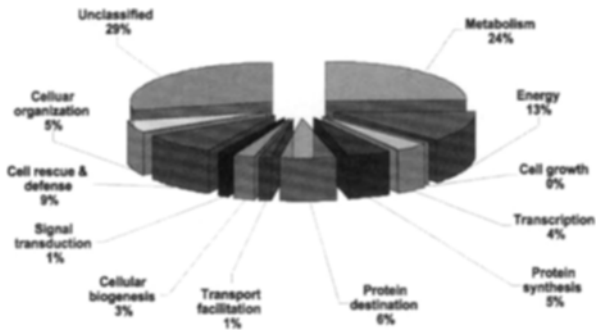

Figure 5. Relative abundance of functionally categorized genes in Type III hairy roots. A total of 79 genes from Table 4 are included. Functional annotation was from either the Munich Information Center for Protein Sequences (MIPS) or the Gene Ontology Consortium.

Sets of genes with reduced expression levels were found in Type III hairy roots that contained very low levels of ginsenosides (Table 4). Of these, 74% are functionally annotated and, interestingly, 24% of them are involved in metabolic functions (Fig. 5). These include several that encode dehydrogenases, transferases, and synthases, and a couple that function in secondary metabolism. Therefore, we can assume that the production of metabolites, including ginsenosides, involves the combined regulation of metabolic genes and heat shock proteins.

Plant Gene Expression during Ginseng Hairy Root Development

Our study provides a proof-of-concept for using the DNA microarray technique to investigate changes in plant gene expression during ginseng hairy root development that had not previously been linked to *A.*

Table 4. Genes with reduced expression levels in type III hairy roots. [a]Function annotation followed either the Munich Information Center for Protein Sequences (MIPS) on the Gene Ontology Consortium.

EST ID	Description	Function[a]
Cluster 4		
PG03008B03	ref|NP_192897.1| (NC_003075) phospholipid hydroperoxide glutathione peroxidase	cell rescue and defense
PG03012G07	emb|CAA59472.1| (X85206) hybrid proline-rich protein	unclassified
Cluster 6		
PG03005D02	ref|NP_176596.1| (NC_003070) hypothetical protein	cell rescue and defense
Cluster 7		
PG03016F09	dbj|BAA96794.1| (AB037421) cytosolic aldehyde dehydrogenase	energy
HJ01022D05	ref|NP_174694.1| (NC_003070) late embryogenesis abundant protein (EMB8)	unclassified
Cluster 8		
HJ01001A06	sp|P31155| S-adenosylmethionine synthase 1	metabolism
PG03014F11	emb|CAA79702.2| (Z21493) mitochondrial formate dehydrogenase precursor	metabolism
PG03004E03	sp|Q9LEJ0| enolase 1 (2-phosphoglycerate dehydrogenase 1)	energy
PG03012B08	emb|CAB39974.1| (AJ133422) glyceraldehyde-3-phosphate dehydrogenase	energy
HJ01004C04	dbj|BAA84650.1| (AB025310) asparaginyl endopeptidase	protein fate
HJ01002D11	ref|NP_000985.1| (NM_000994) ribosomal protein L32; 60S ribosomal protein L32	protein synthesis
HJ01021A07	ref|NP_192897.1| (NC_003075) phospholipid hydroperoxide glutathione peroxidase	cell rescue and defense
PG03015D12	sp|P38546| GTP-binding nuclear protein RAN1	cellular organization
HJ01021F12	gb|AF058955.1|AF058955 Mus musculus ATP-specific succinyl-CoA synthase	unclassified
PG03010C08	gb|AAK06847.1| (AF332565) VirF-interacting protein FIP1	unclassified
PG03015G06	gb|AAK50814.1|AF363286_1 (AF363286) aluminium induced protein	unclassified
PG03014F10	gb|AAK18619.1|AF352797_1 (AF352797) ankyrin-repeat protein HBP1	unclassified
PG03015F03	gb|AAG53944.1| (AF304461) quinone-oxidoreductase QR1	unclassified
PG03015G06	gb|AAK50814.1|AF363286_1 (AF363286) aluminium induced protein	unclassified
Cluster 9		
PG03023F11	ref|NP_189345.1| (NC_003074) gda-1, putative	unclassified
Cluster 10		
HJ01014B03	prf||1804333C Gln synthetase	metabolism
PG03016E06	ref|NP_175202.1| (NC_003070) serpin, putative	protein fate
PG03015D07	ref|NP_173724.1| (NC_003070) unknown protein	unclassified
Cluster 11		
PG03012E06	ref|NP_177067.1| (NC_003070) unknown protein	metabolism
PG03005F04	gb|AAG22740.1|AF282850_1 (AF282850) allergenic isoflavone reductase-like protein	metabolism
PG03024C06	dbj|BAA03710.1| (D16139) cytokinin binding protein CBP57	metabolism
PG03019D06	emb|CAC81811.1| (AJ277278) putative chitinase	cell rescue and defense
Cluster 12		
HJ01014E04	sp|P47916| S-adenosylmethionine synthetase	metabolism
PG03004D05	sp|O22342| ADP,ATP carrier protein 1 precursor	metabolism
PG03002C06	ref|NP_176527.1| (NC_003070) reductase, putative	metabolism
HJ01009C07	ref|NP_180873.1| (NC_003071) 3-ketoacyl-CoA thiolase	energy
HJ01018F10	pir||T07989 acetyl-CoA C-acyltransferase (EC 2.3.1.16) precursor, glyoxysomal	energy
PG03010H10	sp|P26518| glyceraldehyder 3 phosphate dehydrogenase, cytosolic	energy
PG03023H06	gb|AAD28242.1|AF121355_1 (AF121355) peroxiredoxin TPx1	energy
PG03003B01	gb|AAC32162.1| (AF051743) fibrillarin	transcription
HJ01001E09	ref|NP_200539.1| (NC_003076) 60S acidic ribosomal protein P3	protein synthesis
PG03001A06	ref|NP_201552.1| (NC_003076) 60S ribosomal protein L26	protein synthesis
HJ01007A07	gb|AAD34458.1| (AF135596) Skp1	cell cycle
PG03001E07	gb|AAF27340.1|AF186020_1 (AF186020) abscisic acid-activated protein kinase	signal transduction
PG03007A09	gb|AAD47832.1| (AF166332) cytochrome P450	unclassified
PG03007B02	ref|NP_174096.1| (NC_003070) hypothetical protein	unclassified P
G03003D05	sp|Q9XG77| Proteasome subunit alpha type 6 (20S proteasome alpha subunit A)	unclassified
Cluster 13		
HJ01001H10	sp|P11796| Superoxide dismutase	metabolism
HJ01003C04	sp|P31155| S-adenosylmethionine synthetase 1	metabolism
HJ01013F01	ref|NP_172648.1| (NC_003070) lactoylglutathione lyase-like protein	metabolism

Table 4. Continued

EST ID	Description	Function[a]
PG03019B01	sp|P93254| S-adenosylmethionine synthetase	metabolism
PG03003C07	ref|NP_178224.1| (NC_003071) putative aldolase	energy
HJ01018G04	gb|AAL06644.1| (AY048861) putative quinone oxidoreductase	transcription
PG03016A07	ref|NP_188229.1| (NC_003074) putative ribosomal protein	protein synthesis
PG03023E03	gb|AAB51386.1| (U92087) stress responsive cyclophilin	protein fate
HJ01002G10	ref|NP_178970.1| (NC_003071) putative chromodomain-helicase-DNA-binding protein	cell cycle
HJ01001H03	ref|NP_191788.1| (NC_003074) ADP-ribosylation factor-like protein	cellular transport
HJ01022E07	sp|P30175| Actin-depolymerizing factor (ADF)	cellular organization
PG03001D04	gb|AAD24540.1|AF113545_1 (AF113545) vacuole-associated annexin VCaB42	cellular organization
PG03006G07	sp|P09469| Vacuolar ATP synthase catalytic subunit A	cellular organization
HJ01021C05	ref|NP_179311.1| (NC_003071) putative ubiquitin-like protein	unclassified
HJ01022C01	ref|NP_181438.1| (NC_003071) unknown protein	unclassified
PG03002E10	ref|NP_195125.1| (NC_003075) putative protein	unclassified
Cluster 14		
PG03016A11	emb|CAC39216.1| (AJ318053) glutamine synthetas	metabolism
PG03016C01	dbj|BAA34112.1| (AB019327) NADP specific isocitrate dehydrogenase	metabolism
PG03015E12	gb|AAC50019.1| (U39747) high mobility group protein 2 HMG2	transcription
PG03011E01	ref|NP_171732.1| (NC_003070) cathepsin B, putative	protein fate
PG03010H09	dbj|BAB67894.1| (AP003231) putative HSP70	cell rescue and defense
PG03021G11	gb|AAL06644.1| (AY048861) putative quinone oxidoreductase	unclassified
PG03010G12	pir||T15042 omega-6 fatty acid desaturase (EC 1.14.99.-)	unclassified
PG03021F07	sp|Q39182| Gamma-thionin homolog	unclassified
HJ01001F08	ref|NP_520651.1| (NC_003295) probable tetraacyldisaccharide 4-kinase protein	unclassified
Cluster 15		
HJ01019C04	sp|Q9AXE3| S-adenosyl methionine decarboxylase proenzyme	metabolism
PG03013D08	ref|NP_198892.1| (NC_003076) glucose-6-phosphate dehydrogenase	metabolism
PG03015B06	ref|NP_186847.1| (NC_003074) putative dehydrogenase	metabolism
PG03022E03	pir||T14894 glucose-6-phosphate 1-dehydrogenase (EC 1.1.1.49) 1, cytosolic	metabolism
PG03017F03	ref|NP_187337.1| (NC_003074) acetyl-coA dehydrogenase, putative	energy
PG03023H01	ref|NP_199252.1| (NC_003076) berberine bridge enzyme-like protein	energy
HJ01003B03	dbj|BAA87070.2| (AB035272) TAT-binding protein homolog	protein fate
PG03022D01	dbj|BAB40141.1| (AB058678) plasma membrane intrinsic protein 2-1	cellular transport
PG03014D08	gb|AAF44667.1|AF239617_1 (AF239617) beta-1,3-glucanase	cell rescue and defense
PG03014H11	pir||T12249 major latex protein homolog - common ice plant	cell rescue and defense
PG03006A05	ref|NP_190682.1| (NC_003074) putative protein	unclassified
PG03006A07	pir||T15043 fungal elicitor-induced protein parsley	unclassified
PG03008D07	pir||T11576 type IIIa membrane protein cp-wap11 cowpea	unclassified

rhizogenes infection. Although our microarray did not contain all the genes expressed in ginseng roots, our results demonstrated distinctive clustering with possible relevance to hairy root morphology and ginsenoside production. A large number of ribosomal protein genes showed differential expression in the hairy roots that had fewer lateral branches. This phenomenon may provide insight into how the *rol* and *aux* genes in *A. rhizogenes* coordinate with plant genes to orchestrate the process by which hairy roots are initiated and their morphology is determined.

Our results also suggest that two gene groups are responsible for producing the highest level of ginsenosides. These groups represent metabolic genes and those encoding heat shock proteins. Here, the level of expression increased for the latter, while that of the former was reduced in roots that produced more ginsenosides. To an extent, this may reflect a stable environment and the activities of plant growth that are connected with secondary metabolism. However, the biological mechanism through which heat shock proteins are involved in the production of secondary metabolites remains to be clarified. Additional experiments with larger DNA microarrays are currently in progress to specify the gene functions associated with specific metabolic pathways.

ACKNOWLEDGEMENTS

This work was supported by Grant No. PF003101-04 to DWC from the Plant Diversity Research Center of the 21st Century Frontier Research Program, Grant No.

M10104000234-01J000-10710 to JRL from the National Research Laboratory Program, Grant No. BDM0100211 to JRL from the Strategic National R&D Program through the Genetic Resources and Information Network Center, and a grant to JRL from the Korea Science and Engineering Foundation through the Plant Metabolism Research Center of Kyung Hee University funded by the Korean Ministry of Science and Technology. The authors thank Dr. Jong Chan Hong for preparing the cDNA microarray and for his helpful discussion.

Received July 14, 2003; accepted August 11, 2003.

LITERATURE CITED

Amselem J, Tepfer M (1992) Molecular basis for novel phenotypes induced by *Agrobacterium rhizogenes* A4 on cucumber. Plant Mol Biol 19: 421-432

Bonhomme V, Laurain-Mattar D, Lacoux M, Fliniaux J, Jacquin-Dubreuil A (2000) Tropane alkaloid production by hairy roots of *Atropa belladonna* obtained after transformation with *Agrobacterium rhizogenes* 15834 and *Agrobacterium tumefaciens* containing *rol* A, B, C genes only. J Biotech 81: 151-158

Bourgaud F, Gravot A, Milesi S, Gontier E (2001) Production of plant secondary metabolites: An historical perspective. Plant Sci 161: 839-851

Bulgakov V, Khodakovskaya M, Labetskaya N, Chernoded G, Zhuravlev Y (1998) The impact of plant rolC oncogene on ginsenoside production by ginseng hairy root cultures. Phytochemistry 49: 1929-1934

Canto-Canche B, Loyola-Vargas V (1999) Chemicals from roots, hairy roots, and their application. Adv Exp Med Biol 464: 235-275

Giri A, Narasu ML (2000) Transgenic hairy roots: Recent trends and applications. Biotech Adv 8: 1-22

Ito T, Kim GT, Shinozaki K (2000) Disruption of an *Arabidopsis* cytoplasmic ribosomal protein S13-homologous gene by transposon-mediated mutagenesis causes aberrant growth and development. Plant J 22: 257-264

Lian M-L, Chakrabarty D, Paek K-Y (2002) Effect of plant growth regulators and medium composition on cell growth and saponin production during cell-suspension culture of mountain ginseng (*Panax ginseng* C. A. Mayer). J Plant Biol 45: 201-206

Mallol A, Cusido R, Palazon J, Bonfill M, Morales C, Pinol M (2001) Ginsenoside production in different phenotypes of *Panax ginseng* transformed roots. Phytochemistry 57: 365-371

Milioni D, Hatzopoulos P (1997) Genomic organization of hsp90 gene family in *Arabidopsis*. Plant Mol Biol 35: 955-961

Moran DL (2000) Characterization of the structure and expression of a highly conserved ribosomal protein gene, L9, from pea. Gene 253: 19-29

Moyano E, Fornaleb S, Palazona J, Cusidoa RM, Bonfilla M, Moralesa C, Pinola MT (1999) Effect of *Agrobacterium rhizogenes* T-DNA on alkaloid production in Solanaceae plants. Phytochemistry 52: 1287-1292

Nilsson O, Olsson O (1997) Getting to the root: The role of the *Agrobacterium rhizogenes rol* genes in the formation of hairy roots. Physiol Plant 100: 463-473

Palazon J, Cusido RM, Roig C, Pinol MT (1997) Effect of *rol* genes from *Agrobacterium rhizogenes* TL-DNA on nicotine production in tobacco root cultures. Plant Physiol Biochem 35: 155-162

Palazon J, Cusido RM, Roig C, Pinol MT (1998) Expression of the *rolC* gene and nicotine production in transgenic roots and their regenerated plants. Plant Cell Rep 17: 384-390

Park SU, Facchini PJ (2000) *Agrobacterium rhizogenes*-mediated transformation of opium poppy, *Papaver somniferum* L., and California poppy, *Eschscholzia californica* Cham. root cultures. J Exp Bot 51: 1005-1016

Queitsch C, Sangster TA, Lindquist S (2002) Hsp90 as a capacitor of phenotypic variation. Nature 417: 618-624

Shanks JV, Morgan J (1999) Plant 'hairy root' culture. Curr Opin Biotech 10: 151-155

Sodati F (2000) *Panax ginseng* standardization and biological activity, *In* SJ Cutler, HG Cutler, eds, Biologically Active Natural Products: Pharmaceuticals, CRC Press, Washington DC, pp 209-232

Sung DY, Vierling E, Guy CL (2001) Comprehensive expression profile analysis of the *Arabidopsis* Hsp70 gene family. Plant Physiol 126: 789-800

Tanaka N, Yamakawa M, Yamashita I (1998) Characterization of transcription of genes involved in hairy root induction on pRi1724 core-T-DNA in two *Ajuga reptans* hairy root lines. Plant Sci 137: 95-105

Washida D, Shimomura K, Nakajima Y Takido M, Kitanaka S (1998) Ginsenosides in hairy roots of a *Panax* hybrid. Phytochemistry 49: 2331-2335

Weijers D, Dijk MF, Venchen R-J Quint A, Hooykaas P, Offringa R (2001) An *Arabidopsis* Minute-like phenotype caused by semi-dominant mutation in a ribosomal protein S5 gene. Development 128: 4289-4299

Williams ME, Sussex IM (1995) Developmental regulation of ribosomal protein L16 genes in *Arabidopsis thaliana*. Plant J 8: 65-76

Wu J, Zhong JJ (1999) Production of ginseng and its bioactive components in plant cell culture: Current technological and applied aspects. J Biotech 68: 89-99